

Solitary phase waves in a chain of autonomous oscillators

Cite as: Chaos **30**, 053119 (2020); <https://doi.org/10.1063/1.5144939>

Submitted: 13 January 2020 . Accepted: 20 April 2020 . Published Online: 08 May 2020

Philip Rosenau, and Arkady Pikovsky 



View Online



Export Citation



CrossMark

ARTICLES YOU MAY BE INTERESTED IN

[Symmetry breaking dynamics induced by mean-field density and low-pass filter](#)

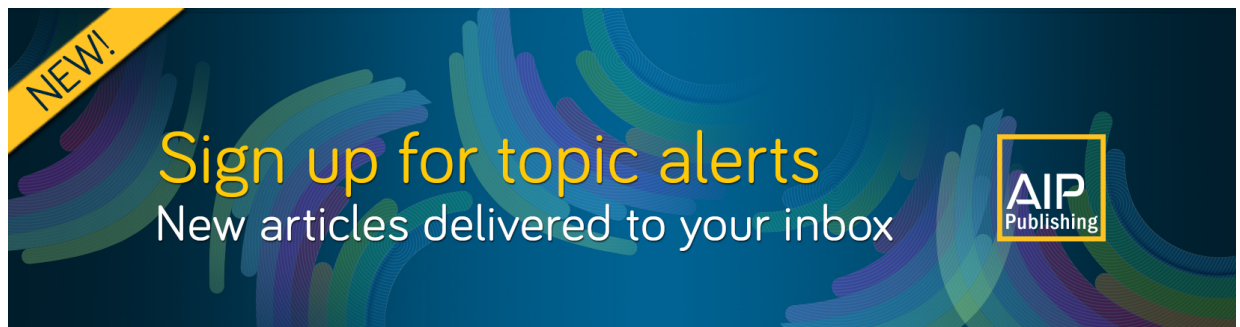
Chaos: An Interdisciplinary Journal of Nonlinear Science **30**, 053120 (2020); <https://doi.org/10.1063/1.5142234>

[Synchronization and spatial patterns in forced swarmalators](#)

Chaos: An Interdisciplinary Journal of Nonlinear Science **30**, 053112 (2020); <https://doi.org/10.1063/1.5141343>

[Adaptive clustering based on element-wised distance for distributed estimation over multi-task networks](#)

Chaos: An Interdisciplinary Journal of Nonlinear Science **30**, 053116 (2020); <https://doi.org/10.1063/1.5141493>



NEW!

Sign up for topic alerts
New articles delivered to your inbox

AIP
Publishing



Solitary phase waves in a chain of autonomous oscillators

Cite as: Chaos 30, 053119 (2020); doi: 10.1063/1.5144939

Submitted: 13 January 2020 · Accepted: 20 April 2020 ·

Published Online: 8 May 2020



View Online



Export Citation



CrossMark

Philip Rosenau¹ and Arkady Pikovsky^{2,3,a)} 

AFFILIATIONS

¹Department of Mathematics, Tel-Aviv University, Tel-Aviv 69978, Israel

²Institute for Physics and Astronomy, University of Potsdam, Karl-Liebknecht-Strasse 24/25, 14476 Potsdam-Golm, Germany

³Laboratory of Dynamical Systems and Applications, HSE University, Bolshaya Pecherskaya St. 25/12, 603155, Nizhny Novgorod, Russia

Note: This article is part of the Focus Issue, instabilities and Nonequilibrium Structures.

a) Author to whom correspondence should be addressed: pikovsky@uni-potsdam.de

ABSTRACT

In the present paper, we study phase waves of self-sustained oscillators with a nearest-neighbor dispersive coupling on an infinite lattice. To analyze the underlying dynamics, we approximate the lattice with a quasi-continuum (QC). The resulting partial differential model is then further reduced to the Gardner equation, which predicts many properties of the underlying solitary structures. Using an iterative procedure on the original lattice equations, we determine the shapes of solitary waves, kinks, and the flat-like solitons that we refer to as flatons. Direct numerical experiments reveal that the interaction of solitons and flatons on the lattice is notably clean. All in all, we find that both the QC and the Gardner equation predict remarkably well the discrete patterns and their dynamics.

Published under license by AIP Publishing. <https://doi.org/10.1063/1.5144939>

Interacting limit cycle oscillators play a fundamental role in synchronization studies. When the coupling is small, system dynamics reduces to that of the oscillator phases. In many setups, as in the seminal Kuramoto model, the interaction is dissipative and leads ultimately to synchrony of all phases. Yet, in many experimental setups, the coupling is dispersive with the resulting phase equations being conservative. We focus on a conservative phase dynamics on a one-dimensional lattice and demonstrate the existence of a very robust dynamics of solitary waves. A crucial role in the understanding of the dynamics is played by its quasi-continuum approximation via a partial differential equation, which provides a remarkably accurate description of the underlying phenomena on the lattice.

I. INTRODUCTION

Dynamics of networks of oscillators have gathered considerable attention in recent years. The dynamics of even the simplest network architectures, such as a global coupling in a population¹ or a local coupling on a regular lattice (see, e.g., Ref. 2), is highly nontrivial even for the simplest Kuramoto–Sakaguchi type of interactions.³

In the latter case, one addresses the phase dynamics of oscillators coupled via their first harmonics with an additional phase shift. This phase shift determines the relative importance of dissipative, diffusion-type, and conservative (dispersive) interactions. For the diffusion-type coupling, the interaction results in global synchronization of a homogeneous lattice. (In an inhomogeneous lattice with random oscillator frequencies, the diffusive coupling should be strong enough to ensure synchrony.⁴) Homogeneous oscillator lattices with a purely conservative coupling follow a very different path for their phase dynamics, which is, surprisingly enough, Hamiltonian, leading to the formation of nontrivial waves, such as compactons or kovatons.^{5–8}

In the present paper, we extend our previous work and address both analytically and numerically a dispersive variant of the Kuramoto–Sagakuchi chain. Studying the solitary structures, we find solitons in a bounded range of velocities. At range's edge, solitons collapse and kink/anti-kink emerge. However, close to the transition's threshold, we find a narrow strip of velocities wherein solitons undergo a structural change, and rather than grow with amplitudes, they widen and turn into flat-top solitons, referred to as flatons. Notably, the interaction between solitons and flatons is found to be remarkably clean.

Next, we mention two potential experimental realizations of dispersive phase oscillator chains. A purely dispersive coupling of self-sustained oscillators, of the type studied here, is relevant in micromechanical oscillators that were studied both theoretically^{9–13} and more recently were explored experimentally.¹⁴ Dispersive coupling of self-sustained oscillators is also relevant in arrays of lasers.^{15,16} In the latter case, typically two-dimensional arrays are explored. Extension of our analysis of a one-dimensional lattice to higher dimensional lattices is a highly nontrivial affair and is left for future studies. In passing, we note that the long chains we have focused on are not easily replicated experimentally. The more realistic short chains where boundary effects matter will also be a subject of future studies.

II. THE BASIC MODEL

Consider a chain of self-sustained, autonomous oscillators with a nearest-neighbor coupling, described via their complex amplitudes A_n ,

$$\frac{dA_n}{dt} = i\omega A_n + \mu A_n(1 - |A_n|^2) + i\varepsilon(A_{n-1} - 2A_n + A_{n+1}). \quad (1)$$

The amplitudes in (1) were normalized with the equilibrium amplitude of a single oscillator being unity, whereas μ , assumed to be large, governs the relaxation rate to the equilibrium so that the limit cycle oscillations are strongly stable. Contrary to the large dissipation of the local amplitude dynamics, the present coupling is assumed to be purely conservative as found in nano-electromechanical setups addressed in Refs. 9–13 and recently realized experimentally.¹⁴ In the $\mu \rightarrow \infty$ limit, one may neglect the changes in amplitude’s modulus and set $A_n = e^{i\varphi_n}$, where φ_n is the phase of the oscillator. This leads to a phase chain model,

$$\frac{d\varphi_n}{dt} = \omega + \varepsilon \left(\cos(\varphi_{n+1} - \varphi_n) + \cos(\varphi_{n-1} - \varphi_n) - 2 \right). \quad (2)$$

In chain (2), any linear phase profile $\varphi_n = (\pi/2 - \alpha)n$ is uniformly rotating (a so-called twisted state¹⁷). To study the deviations from this plane wave, we introduce the phase difference $\theta_n = \varphi_{n+1} - \varphi_n + \alpha - \pi/2$ and rescale the time $\varepsilon t \rightarrow t$ to obtain the following basic model:

$$\frac{d\theta_n}{dt} = \sin(\alpha - \theta_{n+1}) - \sin(\alpha - \theta_{n-1}). \quad (3)$$

As is clear from its derivation, Eq. (3), which is the basis of our studies, describes phase waves on the top of the plane wave, whereas α defines the slope of the background linear phase profile. In particular, the $\alpha = \pi/2$ case was addressed in Refs. 5 and 6.

Noteworthy are the invariance properties of Eq. (3) under $(\theta, \alpha) \rightarrow -(\theta, \alpha)$ and $(\theta, \alpha, n) \rightarrow (-\theta, \pi - \alpha, -n)$ and especially its invariance under

$$\theta \rightarrow 2\alpha - \theta. \quad (4)$$

Consequently, both $\theta = 0$ and $\theta = 2\alpha$ are solutions as is $\theta = \alpha$, which is mapped into itself.

Among the features of Eq. (3), we note the dispersion relation $\omega = 2 \cos \alpha \sin k$, $-\pi \leq k \leq \pi$, of its linear waves and the aforementioned “sonic vacuum” at $\alpha = \pi/2$ ^{5,6} (linear waves are absent),

where the lattice becomes essentially nonlinear. Finally, we note the conservation laws,

$$I_1 = \sum_n \theta_n, \quad I_2 = \sum_n \cos(\alpha - \theta_n), \quad \text{and} \quad I_3 = \sum_n (-1)^n \theta_n, \quad (5)$$

valid on an infinite chain.

III. WAVES IN A QUASI-CONTINUUM

A. General features

In spite of their innocuous appearance, Eq. (3) describes a complicated nonlinear system, which defies a direct analysis. As in previous works,^{5,6,8} to gain insight into its dynamics, we shall adopt a quasi-continuous description wherein the discrete system is replaced with a continuous formulation, which keeps a trace of its discrete origin. To this end, we approximate the chain as $\theta_j(t) \rightarrow \theta(x, t)$ and $f_{j+1} - f_{j-1} \rightarrow 2(f_x + \frac{1}{6}f_{xxx})$, which yields

$$\frac{1}{2} \frac{\partial \theta}{\partial t} + \left(\frac{\partial}{\partial x} + \frac{1}{6} \frac{\partial^3}{\partial x^3} \right) \sin(\theta - \alpha) = 0. \quad (6)$$

As there is no small parameter in the problem, Eq. (6) cannot, in the strict mathematical sense, be considered as an asymptotic description of the discrete problem, and its utility can be judged only *a posteriori*. Nonetheless, both in the present problem and in a large variety of other problems, cf. Refs. 5, 6, and 8, it captures both the qualitative and quantitative properties of the discrete solitary waves remarkably well.

Similarly to the discrete system, Eq. (6) is also invariant under $\theta \rightarrow 2\alpha - \theta$. Thus, if θ_1 is solution so is $\theta_2 = 2\alpha - \theta_1$. This is a cyclic property with θ_2 leading back to θ_1 , and as in the discrete case, the trivial $\theta = 0$ solution yields $\theta = 2\alpha$, whereas $\theta = \alpha$ is mapped into itself.

Separating the linear convection, we rewrite (6) as

$$\frac{1}{2} \theta_t + \cos \alpha \theta_x + C_{qc}(\theta) \theta_x + \frac{1}{6} \frac{\partial^3}{\partial x^3} \sin(\theta - \alpha) = 0, \quad (7)$$

where

$$C_{qc}(\theta) = 2 \sin \left(\frac{\theta}{2} \right) \sin \left(\alpha - \frac{\theta}{2} \right). \quad (8)$$

Note the non-monotone nature of $C_{qc}(\theta)$; it attains its maximal value at $\theta = \alpha$ and vanishes at both $\theta = 0$ and $\theta = 2\alpha$, which merely reflects its invariance under (4).

Equation (6) conserves four local quantities,

$$I_1 = \int \theta dx, \quad I_2 = \int Q(\theta) dx, \quad I_3 = \int \sin \sqrt{6}(x + x_0) \theta dx, \quad (9)$$

$$I_4 = \int \cos \sqrt{6}(x + x_0) \theta dx,$$

where $Q(\theta) = \int \sin(\theta' - \alpha) d\theta' = \cos(\alpha - \theta)$. I_1 and I_2 are in a direct correspondence with the corresponding discrete conservation quantities. Notably, the QC admits also a Lagrangian (for more

details, see Ref. 8),

$$\mathcal{L} = \int \int \left[\frac{1}{2} \psi_x \psi_t - Q(\mathbf{L}\psi_x) \right] dx dt, \quad (10)$$

where

$$\mathbf{L} = \sqrt{1 + \partial_x^2}, \quad \theta = \mathbf{L}v, \quad \text{and} \quad v = \psi_x. \quad (11)$$

Consequently, the QC conserves also the momentum $\int v^2 dx$, and in the original variables,

$$I_5 = \int \theta \mathbf{L}^{-2} \theta dx. \quad (12)$$

B. The Gardner approximation

To unfold the key phenomena, we begin with a weakly nonlinear regime, $\theta \ll 1$, wherein

$$\frac{1}{2} \theta_t + \cos \alpha \theta_x + \left(\frac{\sin \alpha}{2} \theta^2 - \frac{\cos \alpha}{6} \theta^3 \right)_x + \frac{\cos \alpha}{6} \frac{\partial^3 \theta}{\partial x^3} = 0. \quad (13)$$

Note that whereas, on one hand, we have neglected the nonlinear corrections to the third derivative, which, insofar that $\theta - \alpha \neq \pm\pi/2$, has only a minor quantitative impact, on the other hand, to preserve the crucial non-monotone nature of convection, we have carried its expansion to the third order. Using the Galilean invariance to dispense with convection's linear part, after normalization, Eq. (13) begets the celebrated Gardner equation,

$$u_t + C_G(u)u_x + u_{xxx} = 0, \quad \text{where} \quad C_G = 6u(1 - u). \quad (14)$$

Both C_G and Eq. (14) are invariant under $u \rightarrow 1 - u$, which echoes the invariance of the original lattice and its QC rendition under (4). Its solitons, traveling with speed λ , satisfy an ordinary differential equation with respect to $s = x - \lambda t$,

$$\frac{1}{2} u_s^2 + P_G(u) = 0, \quad \text{where} \quad 2P_G(u) = -\lambda u^2 + 2u^3 - u^4. \quad (15)$$

Note that due to the defocusing effect of the cubic term, the potential peaks at $u = \frac{3}{4} [1 + \sqrt{1 - 8\lambda/9}]$ and comes down as the speed increases. Consequently, the resulting solitons,

$$u = \frac{\lambda}{1 + \sqrt{1 - \lambda} \cosh(\sqrt{\lambda}(x - \lambda t))}, \quad (16)$$

have a bounded range of admissible propagation speeds: $0 < \lambda < 1$. At the limiting velocity $\lambda = 1$, potential's peaks touch the u -axis, and the soliton solution (16) flattens into a constant = 1. This is a singular limit at which both kink and an anti-kink form,

$$u = \frac{1}{1 + \exp(\mp s)}, \quad \text{where} \quad s = x - t. \quad (17)$$

Close to the edge of solitons' upper velocity range, there is a narrow strip of velocities where solitons undergo a structural change, and rather than grow with amplitudes, they begin to widen and their top

flattens. To extract these features from Eq. (16), let

$$\lambda_f = 1 - \epsilon^2, \quad \text{where} \quad 0 < \epsilon \ll 1,$$

to obtain

$$u = \frac{1 - \epsilon^2}{1 + \epsilon \cosh[\sqrt{\lambda_f}(x - \lambda_f t)]}, \quad (18)$$

with soliton's amplitude being $u_{\max} = 1 - \epsilon$. The extent of soliton's widening is expressed via $x_{1/2}$, where soliton's amplitude has decreased by half,

$$x_{1/2} \simeq \ln \frac{2}{\epsilon}. \quad (19)$$

Thus, amplitude (velocity) changes $\sim 1 - \epsilon$ ($\sim 1 - \epsilon^2$), which are pretty much numerically unobservable, cause solitons to widen as $\sim \ln 1/\epsilon$. We shall refer to the flat-like solitons as *flatons*.

The proximity of flaton velocities to the edge of the admissible speed range enables approximating them by a kink-anti-kink pair placed at $2x_{1/2} \gg 1$ from each other,

$$u \simeq \frac{1}{1 + \exp(|x| - x_{1/2})}, \quad x \in (-\infty, \infty), \quad (20)$$

and provides an upper bound to all flatons.

C. Analysis of the traveling waves

We now proceed to unfold the solitary wave structure of QC [Eq. (6)]. Seeking traveling waves $\theta = \theta(s = x - \lambda t)$ upon one integration, we have

$$-\frac{\lambda}{2} \theta + \sin(\theta - \alpha) + \sin \alpha + \frac{1}{6} \sin(\theta - \alpha)'' = 0, \quad (21)$$

and, as their small amplitude regime indicates, traveling waves call for $2 \cos \alpha < \lambda$. Integrating Eq. (21), we have

$$\frac{1}{6} \cos^2(\theta - \alpha) \theta_s^2 + P_{qc}(\lambda, \alpha; \theta) = 0, \quad (22)$$

where the potential P_{qc} reads

$$P_{qc}(\lambda, \alpha; \theta) = -\lambda [\theta \sin(\theta - \alpha) + \cos(\theta - \alpha) - \cos \alpha] + [\sin(\theta - \alpha) + \sin \alpha]^2. \quad (23)$$

A typical potential landscape for $\alpha = \pi/4$ is displayed in Fig. 1 for three values of λ . As in the weakly nonlinear case, the bounded potential sets an upper bound at which propagation is possible, corresponding to potential's top descending toward the θ -axis at $\theta = 2\alpha$ with $\lambda = 2 \sin \alpha / \alpha$, where the soliton flattens into a constant and kink/anti-kink emerge. Consequently,

$$2 \cos \alpha = \lambda_{\min} < \lambda < \lambda_{\max} = 2 \frac{\sin \alpha}{\alpha} \quad (24)$$

determines the interval of admissible velocities of solitary waves.

On the basis of the weakly nonlinear regime, we anticipate that as $\lambda \rightarrow \lambda_{\max} = 2 \sin(\alpha)/\alpha$, solitons turn into flatons, which, as illustrated in Fig. 2, is indeed the case.

Note the structural singularity of Eq. (22) at $\theta - \alpha = \pm\pi/2$, denoted by the vertical lines on the potential landscape, where

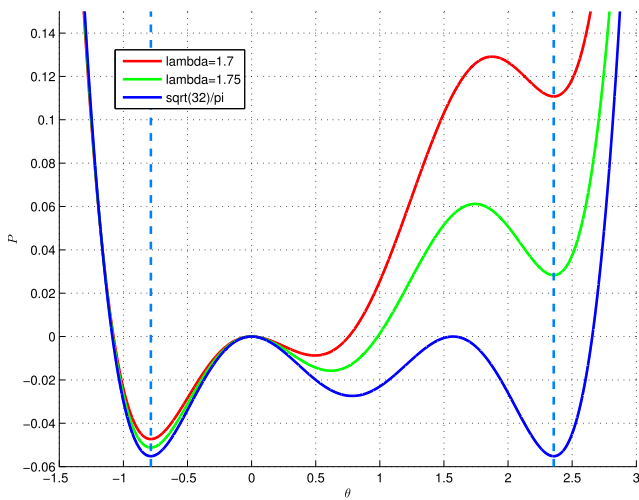


FIG. 1. The potential landscape for $\alpha = \pi/4$ with $(\lambda_{\min}, \lambda_{\max}) = (\sqrt{2}, 4\sqrt{2}/\pi)$. The three plots display the potential corresponding to $\lambda = 1.7, 1.75$, and $4\sqrt{2}/\pi = \lambda_{\max}$. At the critical speed, λ_{\max} potential's positive peak touches the θ -axis, soliton dissolves, and kink/anti-kink connect the two peaks. The two vertical $\theta = \alpha \pm \pi/2$ lines, where Eq. (22) becomes singular, bound the admissible domain.

Eqs. (6) and (22) degenerate, setting $\alpha = \pi/2$ as the highest admissible value of parameter α with the corresponding maximal amplitude $\theta = 2\alpha = \pi$ and the maximal speed of the kink being $\lambda_{\max} = \frac{4}{\pi}$. In the special $\alpha = \pi/2$ case, rather than a sequence of flatons approaching the kink limit, a kovaton emerges, which, since Eq. (6) becomes singular both at $\theta = 0$ and at the top $\theta = \pi$, is and strictly compact there (see Refs. 5 and 6 for a full elaboration of this case). Also, unlike flatons where every width corresponds to a different speed, however minutely different, *all kovatons travel at exactly the*

same limiting velocity of their corresponding kink with their width being chosen at will.

IV. TRAVELING WAVES ON THE CHAIN

Our starting point is the original chain equation (3) rewritten as

$$\begin{aligned} \dot{\theta}_n(t) = \sin \alpha & \left(\cos \theta_{n+1}(t) - \cos \theta_{n-1}(t) \right) \\ & - \cos \alpha \left(\sin \theta_{n+1} - \sin \theta_{n-1} \right). \end{aligned} \quad (25)$$

Seeking traveling waves $\theta_n(t) = \Theta(t - an)$ of Eq. (25), where $a = 1/\lambda$ is the inverse velocity, we obtain an advance-delay equation,

$$\begin{aligned} \dot{\Theta} = \sin \alpha & \left(\cos \Theta(t - a) - \cos \Theta(t + a) \right) \\ & - \cos \alpha \left(\sin \Theta(t - a) - \sin \Theta(t + a) \right). \end{aligned} \quad (26)$$

We integrate Eq. (26) once to obtain

$$\Theta(t) = \int_{t-a}^{t+a} \left[\sin \alpha (1 - \cos \Theta(x)) + \cos \alpha \sin \Theta(x) \right] dx, \quad (27)$$

with the integration constant chosen to assure that $\Theta = 0$ is a solution. In what follows, (27) will be a starting point for the following iterative procedure.

A. Kinks

Assume that there is a kink connecting $\Theta = 0$ with $\Theta = \Theta_0$. Setting $\Theta = \Theta_0$ in (27) begets a condition relating a with Θ_0 ,

$$\Theta_0 = 2a[\sin \alpha - \sin(\alpha - \Theta_0)]. \quad (28)$$

However, symmetry (4) dictates that for a given inverse velocity a , there should be a solution connecting $\Theta_1 = 2\alpha$ with $\Theta_2 = 2\alpha - \Theta_0$.

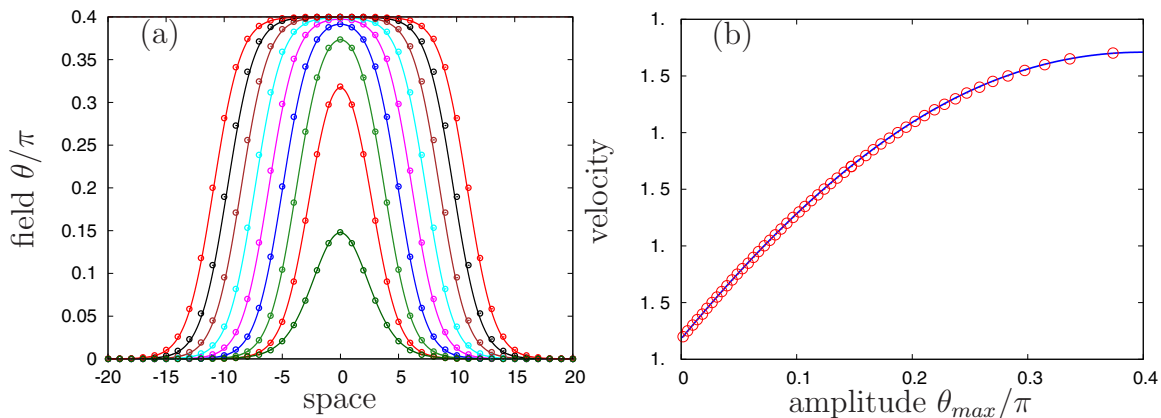


FIG. 2. Waves for $\alpha = 0.2\pi$. (a) Solitary solutions of the chain, Eq. (32) (circles), superimposed on the QC rendition, Eq. (22), for different values of their velocity deviations from its upper bound. From bottom to top: $\lambda_{\max} - \lambda = 10^{-m}$, $m = 1, \dots, 9$. (b) Velocity of solitons vs their amplitude in both discrete and QC renditions. Observe the remarkable fit between the QC and its discrete antecedent.

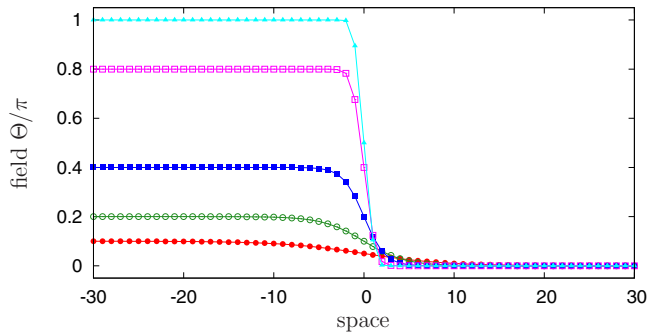


FIG. 3. Discrete kinks for different values of α from bottom to top $\alpha = 0.05\pi, 0.1\pi, 0.2\pi, 0.4\pi,$ and 0.5π . In the last, exceptional, case, the tail decays at a double exponential rate.

This leads to an additional condition relating a and Θ_0 ,

$$2\alpha = 2a[\sin \alpha - \sin(\alpha - 2\alpha)] = 4a \sin \alpha, \tag{29}$$

$$2\alpha - \Theta_0 = 2a[\sin \alpha - \sin(\alpha - 2\alpha + \Theta_0)] = 2a[\sin \alpha - \sin(\Theta_0 - \alpha)]. \tag{30}$$

Adding (28) and (30), we have

$$2\alpha = 4a \sin \alpha,$$

which coincides with the λ_{\max} derived in Sec. III C. Using $a = \frac{\alpha}{2 \sin \alpha}$ in (30), we have

$$\frac{\sin(\Theta_0 - \alpha)}{\Theta_0 - \alpha} = \frac{\sin \alpha}{\alpha},$$

with the obvious solution $\Theta_0 = 2\alpha$, which may serve as kink’s amplitude.

To determine the kink, we solve Eq. (27) iteratively,

$$\Theta^{(k+1)}(t) = \int_{t-a}^{t+a} [\sin \alpha (1 - \cos \Theta^{(k)}(x)) + \cos \alpha \sin \Theta^{(k)}(x)] dx. \tag{31}$$

Starting from an initial ansatz $\Theta^{(0)}(x)$, having a proper asymptotic behavior at $x \rightarrow \pm\infty$, these iterations converge and yield the kink profiles shown in Fig. 3.

B. Solitary waves

In order to apply the iterative procedure due to Petviashvili^{18,19} to solitary waves and to avoid convergence to the trivial solution, we modify it by introducing an intermediate normalization step,

$$\begin{aligned} \tilde{\Theta}(t) &= \int_{t-a}^{t+a} [\sin \alpha (1 - \cos \Theta^{(k)}(x)) + \cos \alpha \sin \Theta^{(k)}(x)] dx, \\ \Theta^{(k+1)} &= \left(\frac{\|\Theta^{(k)}\|}{\|\tilde{\Theta}\|} \right)^\gamma \tilde{\Theta}, \end{aligned} \tag{32}$$

where $\|\diamond\|$ stands for any norm (in our implementation, the L_1 -norm was used). Also, to assure a faster convergence, the exponent $1 < \gamma \leq 2$ was adjusted to the assumed α and a (though the convergence itself does not depend on γ). When carrying the iterations (32), we fix α and a and start with a solitary profile. The resulting iterations yield a solitary solution on the chain. In Fig. 2, we compare the discrete solitary solutions with the corresponding QC solitary solutions obtained solving Eq. (22) and, as clearly seen, find a remarkable overlap attesting to the utility of the QC rendition.

It is instructive to represent the solitary waves in terms of the original phases φ_n rather than in the phase differences θ_n [cf. Eqs. (2) and (3)]. This is done in Fig. 4, where we have adopted the reference frame with $\omega = 0$.

V. DIRECT SIMULATIONS OF THE CHAIN

We now proceed to present the results of our direct simulations of the chain (25). We address two basic initial-value problems.

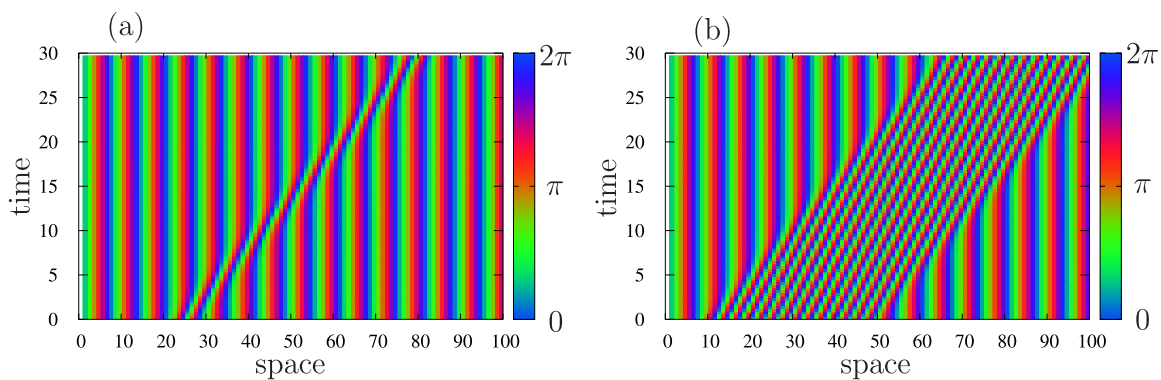


FIG. 4. Space–time plots of a soliton [panel (a)] and of a flaton [panel (b)] in terms of the phases $\varphi_n(t)$ (color-coded values) for $\alpha = 0.2\pi$. The background stripes represent the plane wave on the base of which solitary waves propagate.

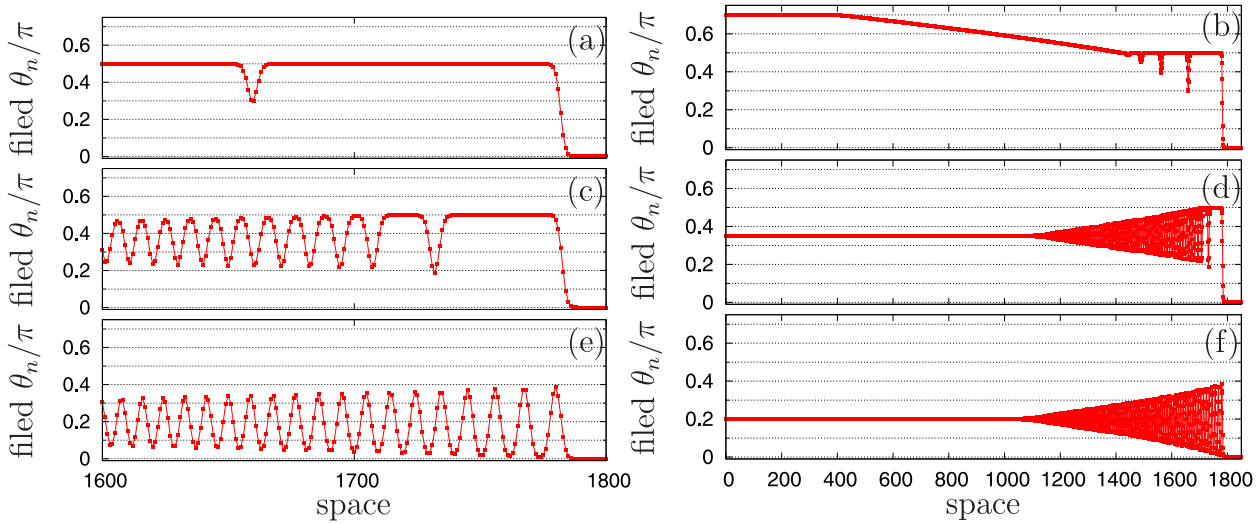


FIG. 5. $\alpha = 0.25\pi$. Evolution on the lattice for different downstream values of A —panels (a) and (b): $A = 0.7\pi$, panels (c) and (d): $A = 0.35\pi$, and panels (e) and (f): $A = 0.2\pi$. The left panel enlarges the vicinity of the front.

A. Evolution of an initial step

Consider an initial step profile $\theta_n(0) = \frac{A}{2}(1 - \tanh \frac{4(n-n_0)}{N_0})$ with $N_0 = 50$, connecting downstream A with the trivial upstream, and follow the frontal edge of the propagating wave. Figure 5 displays three different evolution scenarios according to order relations between the downstream amplitude A and α .

1. $A > 2\alpha$; as seen in Figs. 5(a) and 5(b), a kink forms. It is followed by a characteristic linear profile connecting downstream A with kink’s amplitude 2α . Behind kink’s leading profile, a few solitons emerge, which, due to the invariance (4), point down from the top plateau 2α . Being much slower than the kink, they lag far behind the emerging dispersionless profile.

2. $\alpha \lesssim A \lesssim 2\alpha$. As seen in Figs. 5(c) and 5(d), a kink forms, but now, it is followed by an oscillating domain with a nearly triangular envelope, which intermediates between the downstream A and kink’s frontal amplitude 2α . The waves-train can be viewed as a sequence of negative solitons, though in Figs. 5(c) and 5(d), only the first few pulses have become truly isolated pointing-down solitons.

3. $A \lesssim \alpha$ [see Figs. 5(e) and 5(f)]. A kink does not form. Instead, there is a wave packet embedded within a triangular envelope. In the course of the evolution, the leading waves continue to separate from each other to become true solitons with the leading amplitude $\approx 2A$ propagating with a velocity as given via $P_{qc}(\lambda; \frac{\pi}{2}, 2A) = 0$.

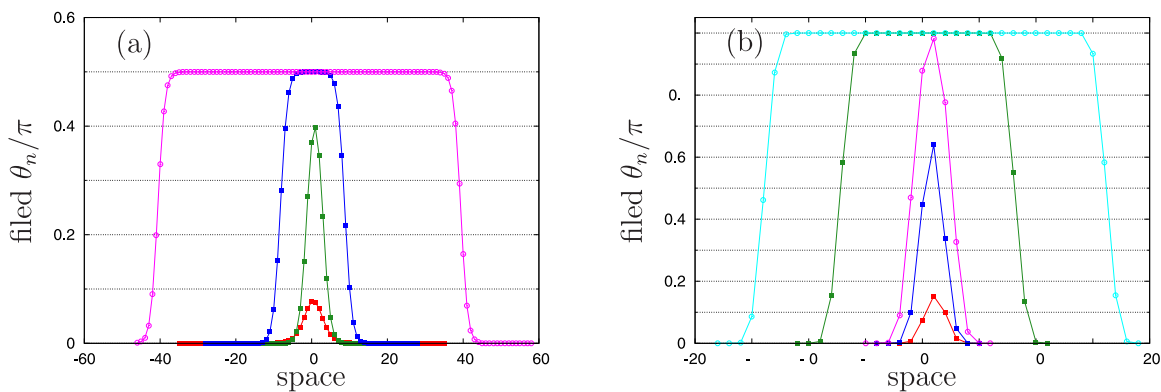


FIG. 6. Emergence of flatons and kovatons. Panel (a): $\alpha = 0.25\pi$ and from bottom to top: $A = 0.05, 0.25, 0.5$, and 1.5 . Panel (b): $\alpha = 0.5\pi$ and from bottom to top: $A = 0.05, 0.4, 0.6, 1.0$, and 1.5 . The difference between the two, though unobservable to the eye, is meaningful. Whereas flaton’s tails decay exponentially, kovaton’s tails decay at a doubly exponential rate, which reflects the fact that in the QC limit, it has a strictly compact support.

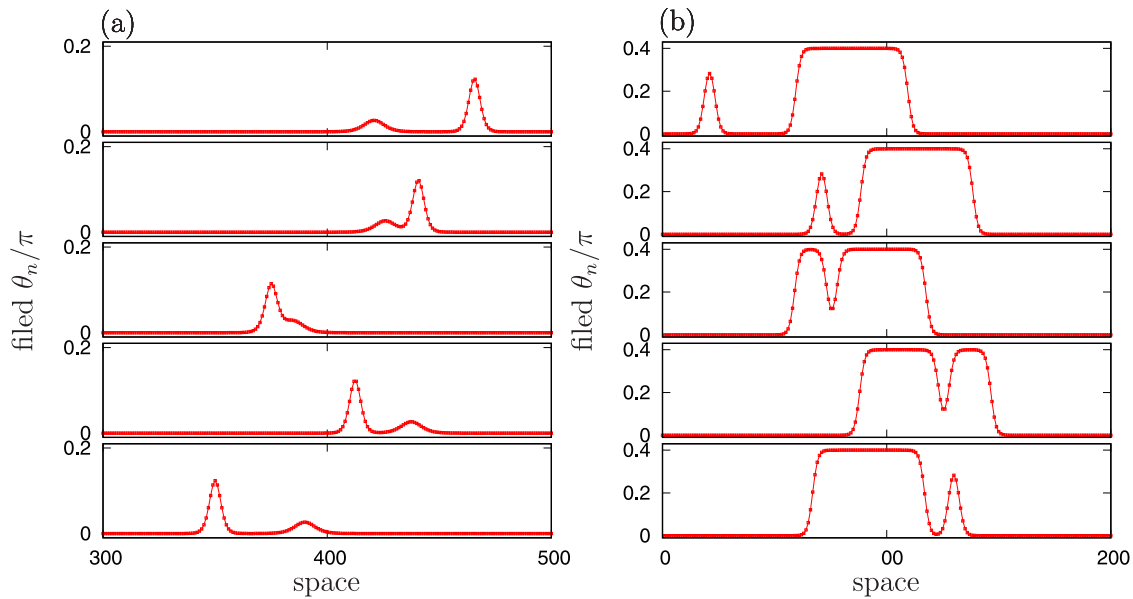


FIG. 7. Interaction of waves for $\alpha = 0.2\pi$. Panel (a): Interaction of two solitons. Panel (b): interaction of a flaton with a soliton. The interval between the frames (starting from the bottom) is $\Delta t = 150$. The profiles are arbitrarily shifted in the n -direction.

We now append the above phenomenological description of the numerical simulations with an analysis based on the remarkable proximity we have found between the dynamics on the lattice, its QC rendition, and the Gardner equation. To this end, we shall refer to the recent study of the Gardener equation by Kamchatnov *et al.*²⁰ and to an earlier seminal work of Gurevich and Pitaevskii.²¹ The comparison is based on their analysis of the signaling problem for Eq. (14),

$$u(x, 0) = \begin{cases} A & \text{for } x < 0, \\ 0 & \text{for } x > 0. \end{cases} \quad (33)$$

We start noting (the parentheses refer to the corresponding QC case) that the convection $C_G = 6u(1 - u)$ ($C_{eq}(\theta) = 2 \sin(\frac{\theta}{2}) \sin(\alpha - \frac{\theta}{2})$) has three key points: $u = 0$ ($\theta = 0$) and $u = 1$ ($\theta = 2\alpha$), where it vanishes, and a turning point where it attains its maximal value, which separates the two domains of monotonicity at $u = 1/2$ in Gardner’s case and $\theta = \alpha$ in the QC.

With the upstream being trivial, according to Ref. 20, there are three regimes according to the position of the downstream amplitude A vs the three key points:

- (1) $A < 1/2$ (QC: $A < \alpha$),
- (2) $1/2 < A < 1$ (QC: $\alpha < A < 2\alpha$), and
- (3) $1 < A$ (QC: $2\alpha < A$).

We now detail the dynamics of Gardner’s equation vis-à-vis the numerical results, in parentheses, in the various regimes.

- (1) $A < 1/2$ (QC: $A < \alpha$). The downstream and the upstream are on the same side of the monotonicity. In this regime, the Gard-

ner equation is de facto governed by the KdV equation to which it reduces when the cubic term becomes secondary. Consequently, as follows from the analysis in Refs. 20 and 21, the solution takes the form of a modulated periodic wave, the so-called undular bore, with a lead amplitude having twice its downstream value, i.e., $2A$; see Fig. 6 in Ref. 20. So much for Gardner, returning to our case, panels (e)–(f) in Fig. 5 clearly show that the analytical features displayed by Gardner’s equation parallel the simulation results of the chain!

- (2) $1/2 < A < 1$ (QC: $\alpha < A < 2\alpha$). The downstream and the upstream are now on the opposite sides of convection’s monotonicity, and Gardner’s solution consists of two parts; let $u(*) = 1$ ($\theta(*) = 2\alpha$) be the point where convection vanishes, then, provided that $A < u(*)$, instead of a single modular kink spanning, as in the previous case, the whole upstream–downstream range, we now have a reverse modular kink connecting the downstream state A with an intermediate state $u(*)$, which then connects to the trivial upstream via a kink; see Fig. 8 in Ref. 20. Exactly the same phenomenon is seen on panels (c) and (d) of Fig. 5, where $\theta(*) = 2\alpha$. [That $u(*) = 1$ is a consequence of the upstream being trivial. If $0 < u(+\infty) < 1/2$, $u(*) = 1 - u(+\infty)$, and kink’s amplitude depends on $u(+\infty)$ as well.²⁰]
- (3) $1 < A$ (QC: $2\alpha < A$). This is a dispersionless regime, and rather than a modulated periodic wave, we have a rarefaction wave that intermediates between the downstream A and a kink at the front, propagating with the highest admissible velocity; see Fig. 10 in Ref. 20. Exactly the same effect is observed in panels (a) and (b) of the chain, with 2α being kink’s amplitude.

B. Evolution of an initial pulse

This is arguably the most basic numerical experiment. We follow the evolution of an initially single pulse excitation $\theta_n(0) = \frac{A}{\cosh^2 \frac{4(n-n_0)}{N_0}}$, with $N_0 = 50$. It begets a sequence of solitary waves with the leading waves being, for small A , solitons, which turn into flatons for large A 's; see the left plate in Fig. 6 and kovatons in the right plate. Though in these simulations flatons and kovatons emerge very naturally, emergence of several flatons or kovatons was never observed, with the solitons forming behind the leading flaton/kovaton having amplitudes smaller than 2α and thus slower as well. Notably, the Gardner equation, which served us so well in the signaling problem, does not beget flatons easily in the corresponding numerical experiments.²² They seem to have a very narrow domain of attraction, and for a flaton to emerge, a special "tailoring" of initial data was necessary, though once present, they have all the features of an integrable entity.

C. Interaction of solitary waves

The essence of our findings is summarized in Fig. 7, which displays collisions of two solitons and a collision of a flaton with a soliton: both in Fig. 7 and other numerical experiments, we have carried, the interaction on the lattice of solitary waves, whether solitons or flatons, is remarkably clean, and the interacting entities re-emerge without visible distortion or radiation.

VI. SUMMARY

In this paper, we have explored the emergence and interaction of nonlinear traveling waves in a phase oscillator chain. We have found, both for the quasi-continuous rendition and its discrete antecedent, a variety of soliton and kink solutions. Furthermore, we have found that solitons in a velocity range close to kinks flatten and become very wide. We thus refer to such solitons as flatons. In 1D, flatons can be looked upon as a joined pair of two kinks. *In direct numerical simulations of the chain, we have seen the flatons emerging out of a variety of large initial excitations.* Notably, the interaction of solitons and solitons with a flaton are very clean and without a noticeable distortion or radiation.

Finally, we reiterate both the remarkable roles of the Gardner equation (14), which was deduced at a second stage of approximation of the chain, in unfolding the various facets of the dynamics and the actual affinity between its patterns and the patterns both observed on the chain and predicted by its QC rendition.

ACKNOWLEDGMENTS

The authors thank M. Matheny and L. Smirnov for useful discussions. A.P. is supported in part by the Laboratory of Dynamical

Systems and Applications NRU HSE of the Ministry of Science and Higher Education of Russian Federation (Grant Agreement No. 075-15-2019-1931).

REFERENCES

- ¹A. Pikovsky and M. Rosenblum, "Dynamics of globally coupled oscillators: Progress and perspectives," *Chaos* **25**, 097616 (2015).
- ²S. Yanchuk and M. Wolfrum, "Destabilization patterns in chains of coupled oscillators," *Phys. Rev. E* **77**, 026212 (2008).
- ³H. Sakaguchi and Y. Kuramoto, "A soluble active rotator model showing phase transition via mutual entrainment," *Prog. Theor. Phys.* **76**, 576–581 (1986).
- ⁴G. B. Ermentrout and N. Kopell, "Frequency plateaus in a chain of weakly coupled oscillators, I," *SIAM J. Math. Anal.* **15**, 215–237 (1984).
- ⁵P. Rosenau and A. Pikovsky, "Phase compactons in chains of dispersively coupled oscillators," *Phys. Rev. Lett.* **94**, 174102 (2005).
- ⁶A. Pikovsky and P. Rosenau, "Phase compactons," *Physica D* **218**, 56–69 (2006).
- ⁷K. Ahnert and A. Pikovsky, "Traveling waves and compactons in phase oscillator lattices," *Chaos* **18**, 037118 (2008).
- ⁸P. Rosenau and A. Zilburg, "Compactons," *J. Phys. A Math. Theor.* **51**, 343001 (2018).
- ⁹M. C. Cross, A. Zumdieck, R. Lifshitz, and J. L. Rogers, "Synchronization by nonlinear frequency pulling," *Phys. Rev. Lett.* **93**, 224101 (2004).
- ¹⁰M. C. Cross, J. L. Rogers, R. Lifshitz, and A. Zumdieck, "Synchronization by reactive coupling and nonlinear frequency pulling," *Phys. Rev. E* **73**, 036205 (2006).
- ¹¹T. E. Lee and M. C. Cross, "Pattern formation with trapped ions," *Phys. Rev. Lett.* **106**, 143001 (2011).
- ¹²M. H. Matheny, M. Grau, L. G. Villanueva, R. B. Karabalin, M. C. Cross, and M. L. Roukes, "Phase synchronization of two anharmonic nanomechanical oscillators," *Phys. Rev. Lett.* **112**, 014101 (2014).
- ¹³W. Fon, M. H. Matheny, J. Li, L. Krayzman, M. C. Cross, R. M. D'Souza, J. P. Crutchfield, and M. L. Roukes, "Complex dynamical networks constructed with fully controllable nonlinear nanomechanical oscillators," *Nano Lett.* **17**, 5977–5983 (2017).
- ¹⁴M. H. Matheny, J. Emenheiser, W. Fon, A. Chapman, A. Salova, M. Rohden, J. Li, M. Hudoba de Bady, M. P'osfai, L. Duenas-Osorio, M. Mesbahi, J. P. Crutchfield, M. C. Cross, R. M. D'Souza, and M. L. Roukes, "Exotic states in a simple network of nanoelectromechanical oscillators," *Science* **363**, eaav7932 (2019).
- ¹⁵M. Nixon, E. Ronen, A. A. Friesem, and N. Davidson, "Observing geometric frustration with thousands of coupled lasers," *Phys. Rev. Lett.* **110**, 184102 (2013).
- ¹⁶M. Fridman, M. Nixon, N. Davidson, and A. A. Friesem, "Coherent combining and phase locking of fiber lasers," in *Coherent Laser Beam Combining*, edited by A. Brignon (Wiley, 2013), Chap. 12, pp. 371–400.
- ¹⁷D. A. Wiley, S. H. Strogatz, and M. Girvan, "The size of the sync basin," *Chaos* **16**, 015103 (2006).
- ¹⁸V. I. Petviashvili, *Sov. J. Plasma Phys.* **2**, 257 (1976).
- ¹⁹V. I. Petviashvili, "Multidimensional and dissipative solitons," *Physica D* **3**, 329–334 (1981).
- ²⁰A. M. Kamchatnov, Y.-H. Kuo, T.-C. Lin, T.-L. Horng, S.-C. Gou, R. Clift, G. A. El, and R. H. J. Grimshaw, "Undular bore theory for the Gardner equation," *Phys. Rev. E* **86**, 036605 (2012).
- ²¹A. V. Gurevich and L. P. Pitaevskii, "Nonstationary structure of a collisionless shock wave," *J. Exp. Theor. Phys.* **38**, 291–297 (1974).
- ²²P. Rosenau and A. Oron, "Flatons: flat-top solitons in extended Gardner-like equations," *Commun. Nonl. Sci. Num. Simul.* (submitted) (2020).